Reologie is overal (part 2)

WND Conferentie, Noordwijkerhout
16, 17 december 2011

Gerrit W.M. Peters

Technische Universiteit
Eindhoven
University of Technology

Where innovation starts

three cases

- case 1: brain tissue (biomechanics)
- case 2: carnivorous plant (biology)
- case 3: semi-crystalline polymers (polymer physics)

introduction: traumatic brain injury

- large deformation (strain) → Traumatic Brain Injury (TBI)
- often occur during rotational and translational acceleration of the head
- exact mechanism of TBI still incompletely understood

introduction: traumatic brain injury

- Injury assessment (industry):
  - anthropomorphic test devices (ATD)
  - Head Injury Criterion (HIC)

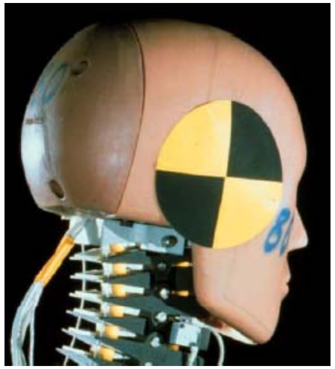

global head load

Head Injury Criterion

$$HIC = \left\{ (t_2 - t_1) \left[\frac{1}{(t_2 - t_1)} \int_{t_1}^{t_2} a(t) \mathrm{d}t \right]^{2.5} \right\}_{\max}$$

brain damage

introduction: traumatic brain injury

- Injury assessment (industry):
  - anthropomorphic test devices (ATD)
  - Head Injury Criterion (HIC)

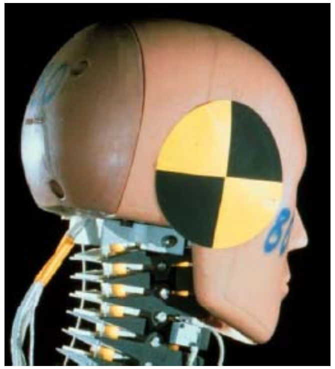

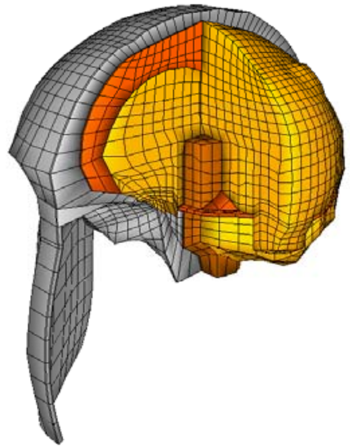

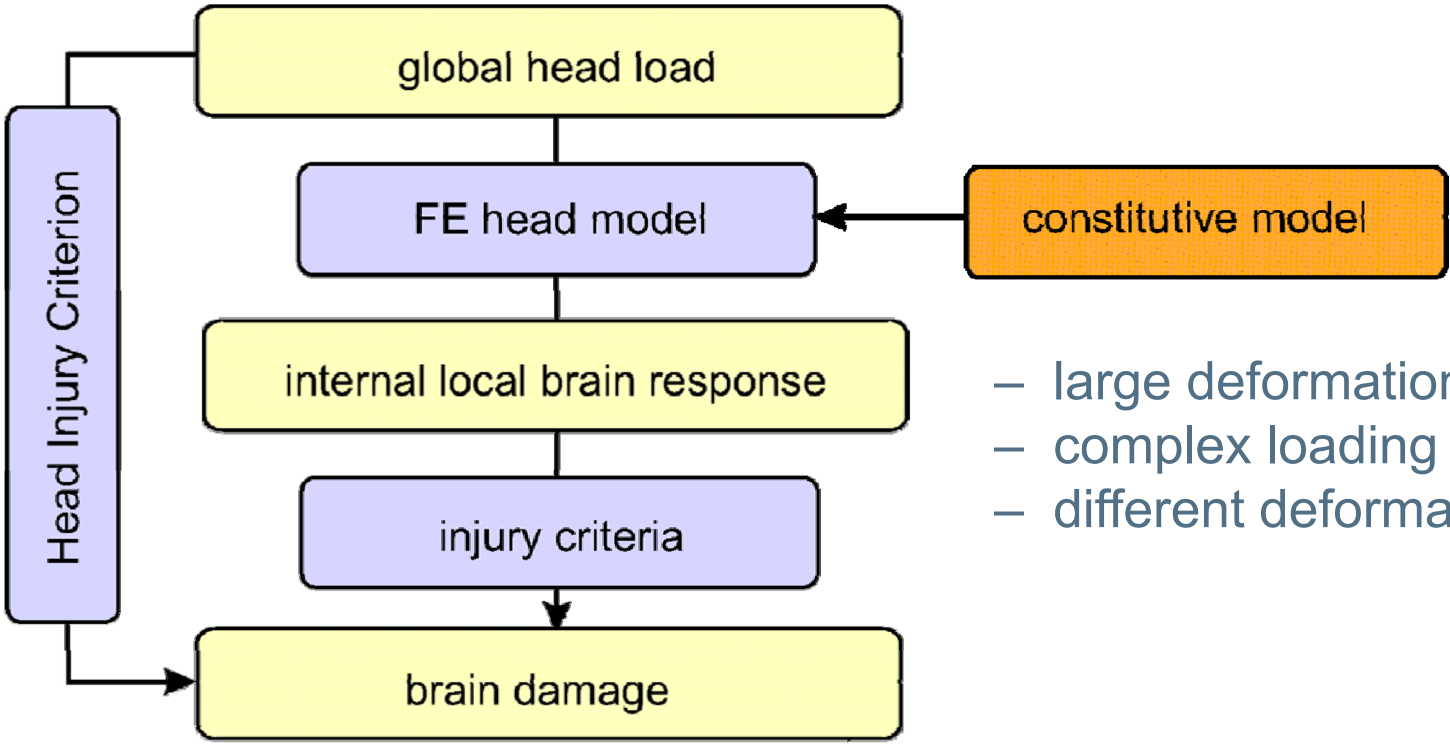

- large deformations
- complex loading paths
- different deformation modes

brain deformations: experiment

test device (high speed loading)

brain deformations: experiment

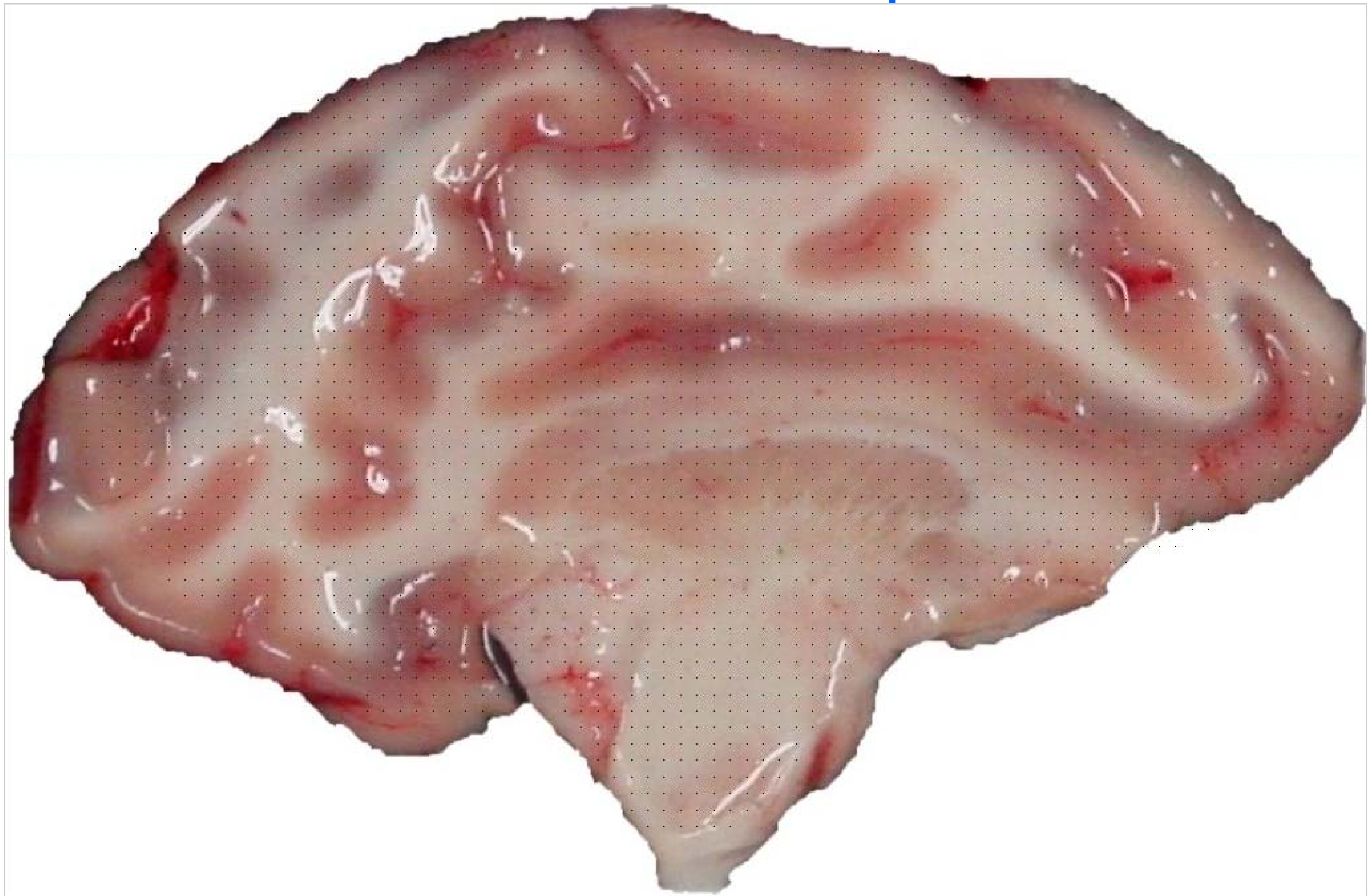

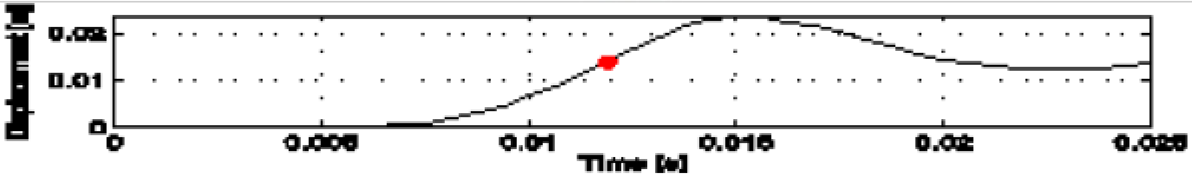

brain deformations: experiment / simulations

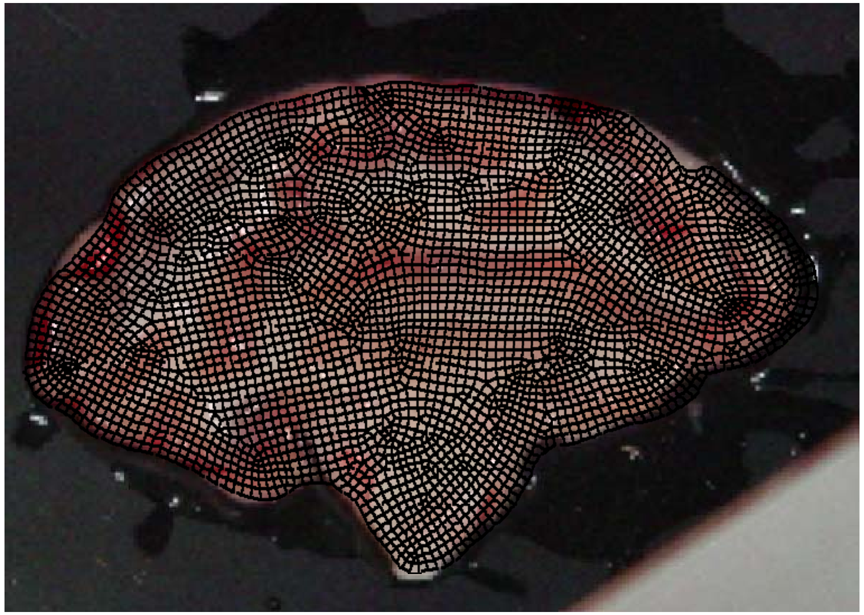

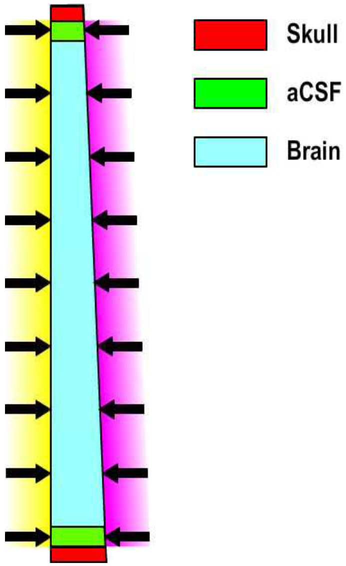

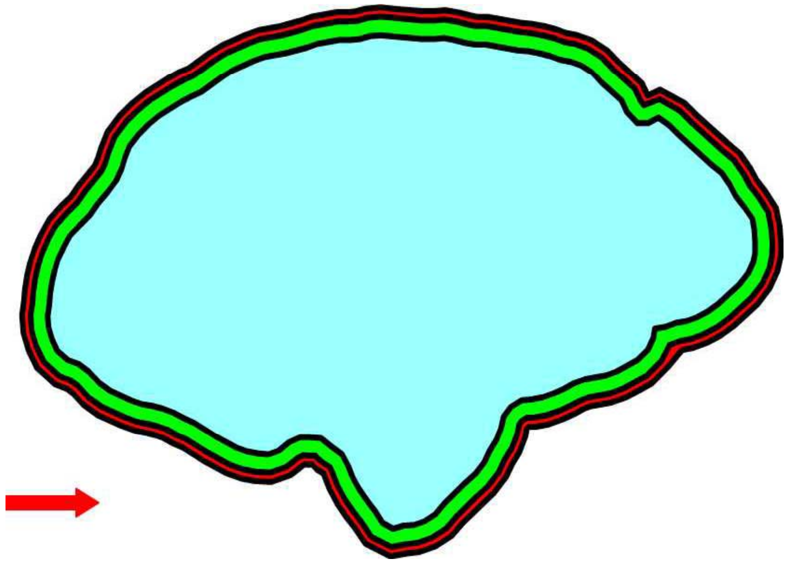

brain deformations: experiment / simulations

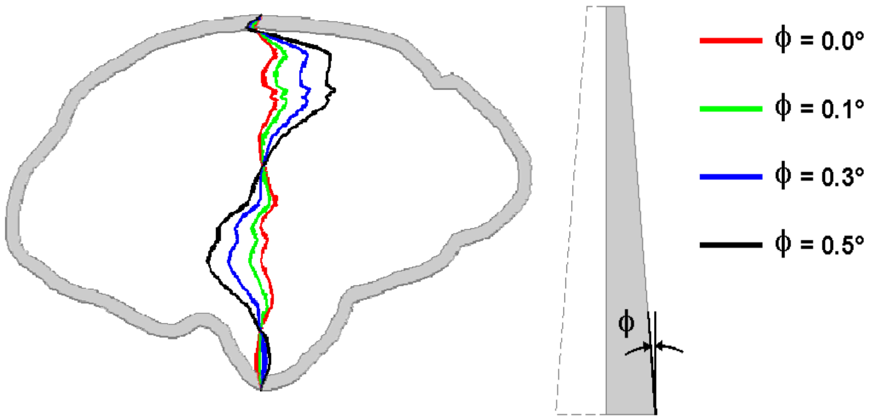

Simulations | Experiment

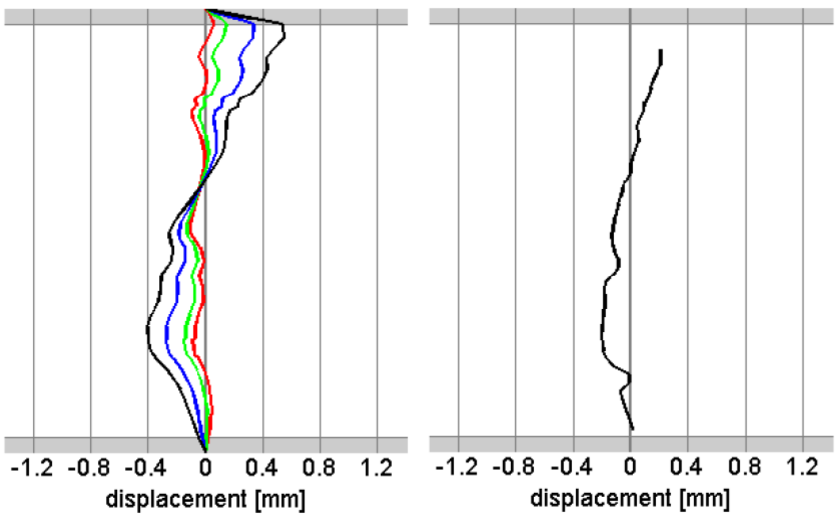

t = 8 ms

Simulations | Experiment

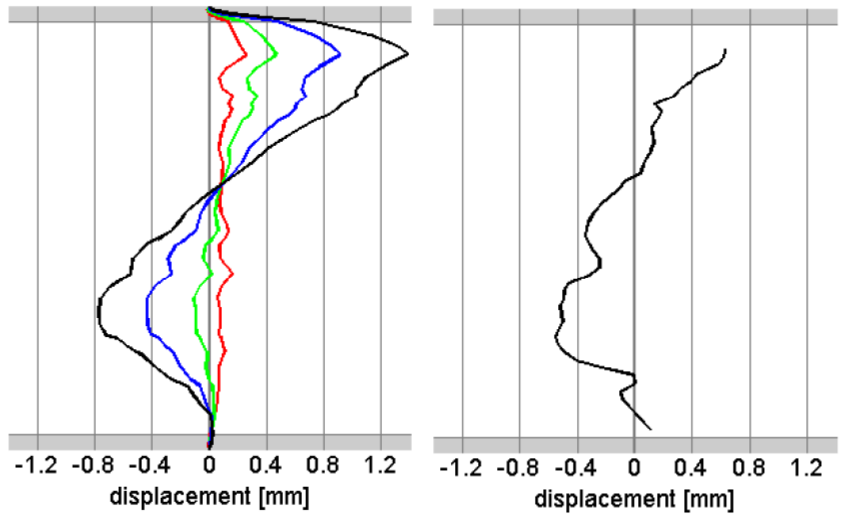

t = 12 ms

model application

Current model

Brands et al. model

Current model simplified

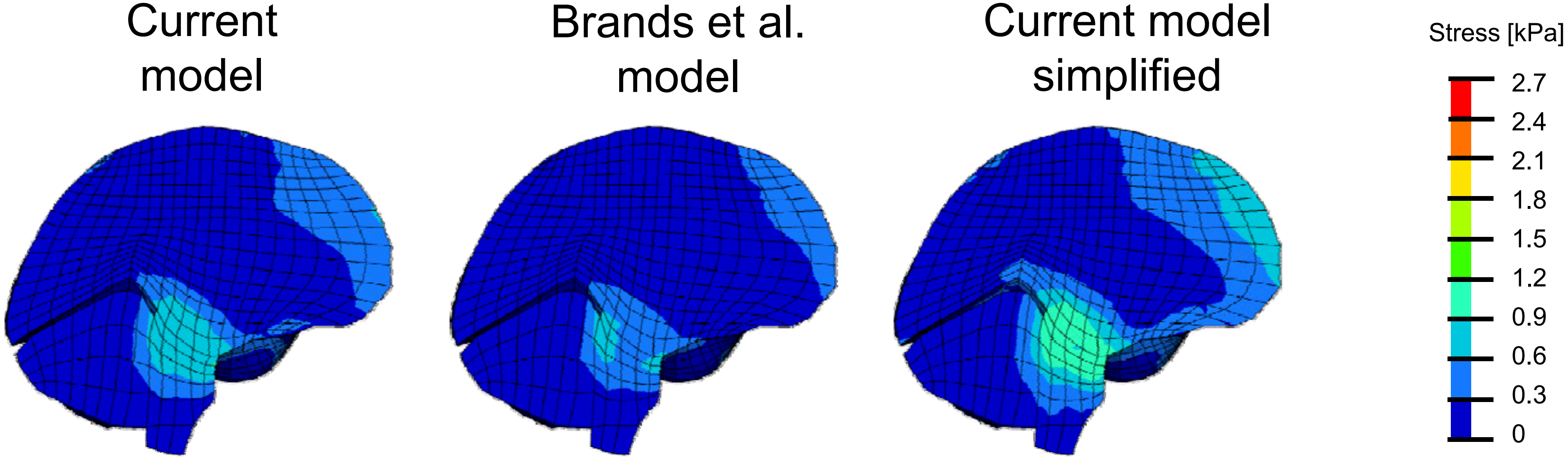

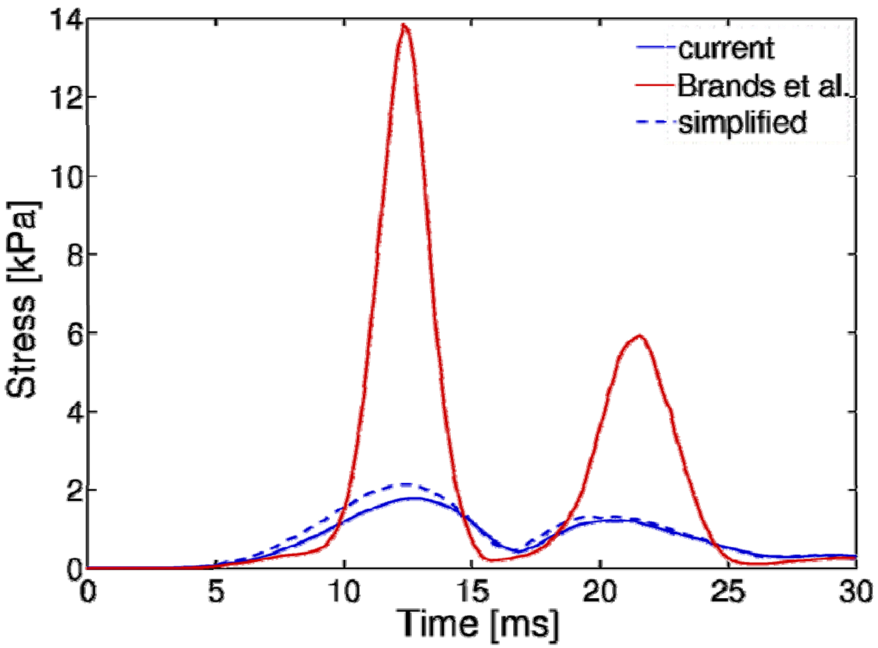

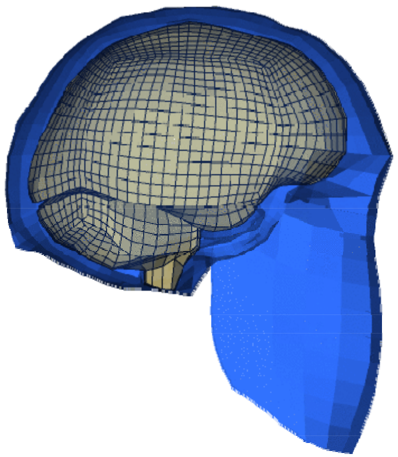

model application

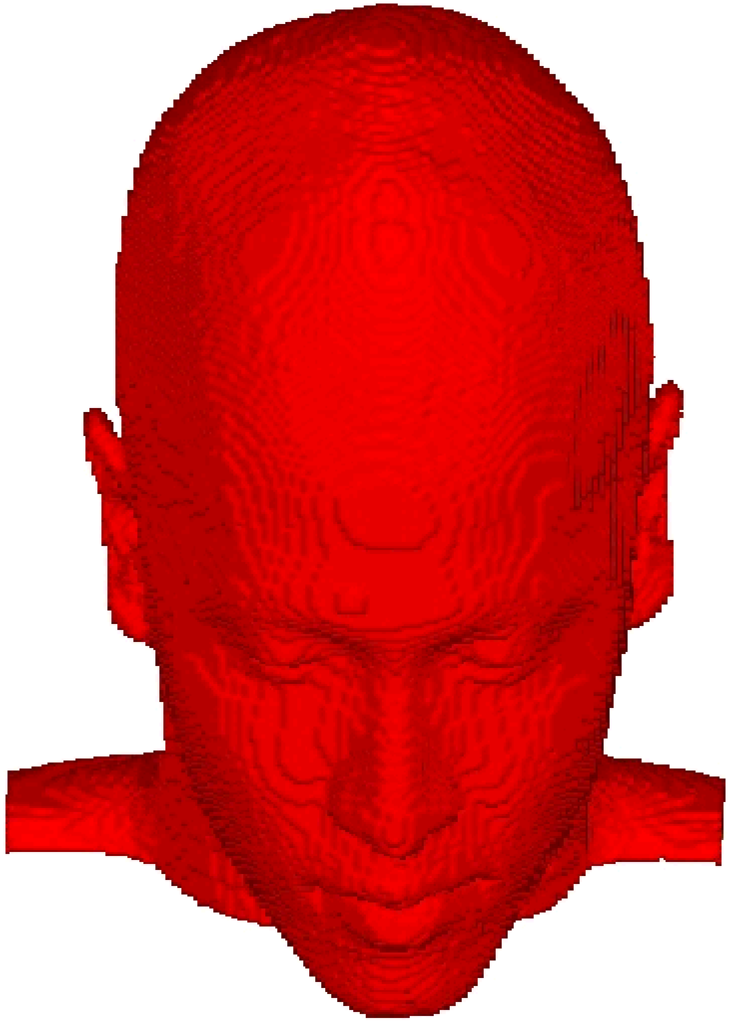

model application

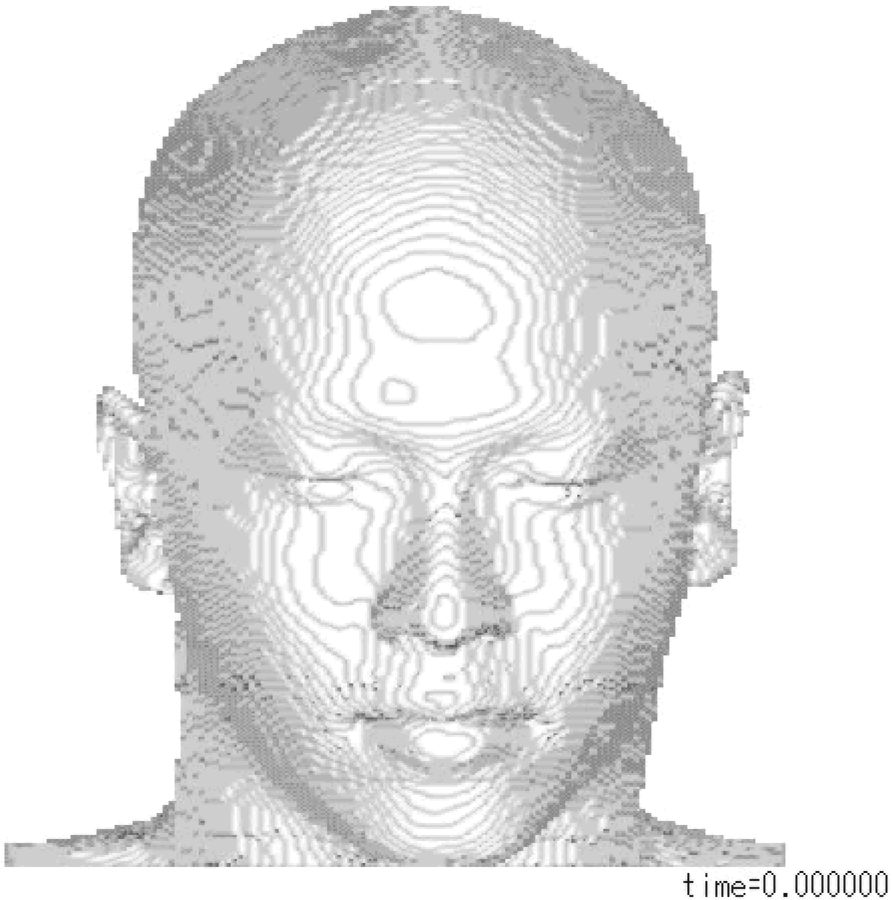

model application

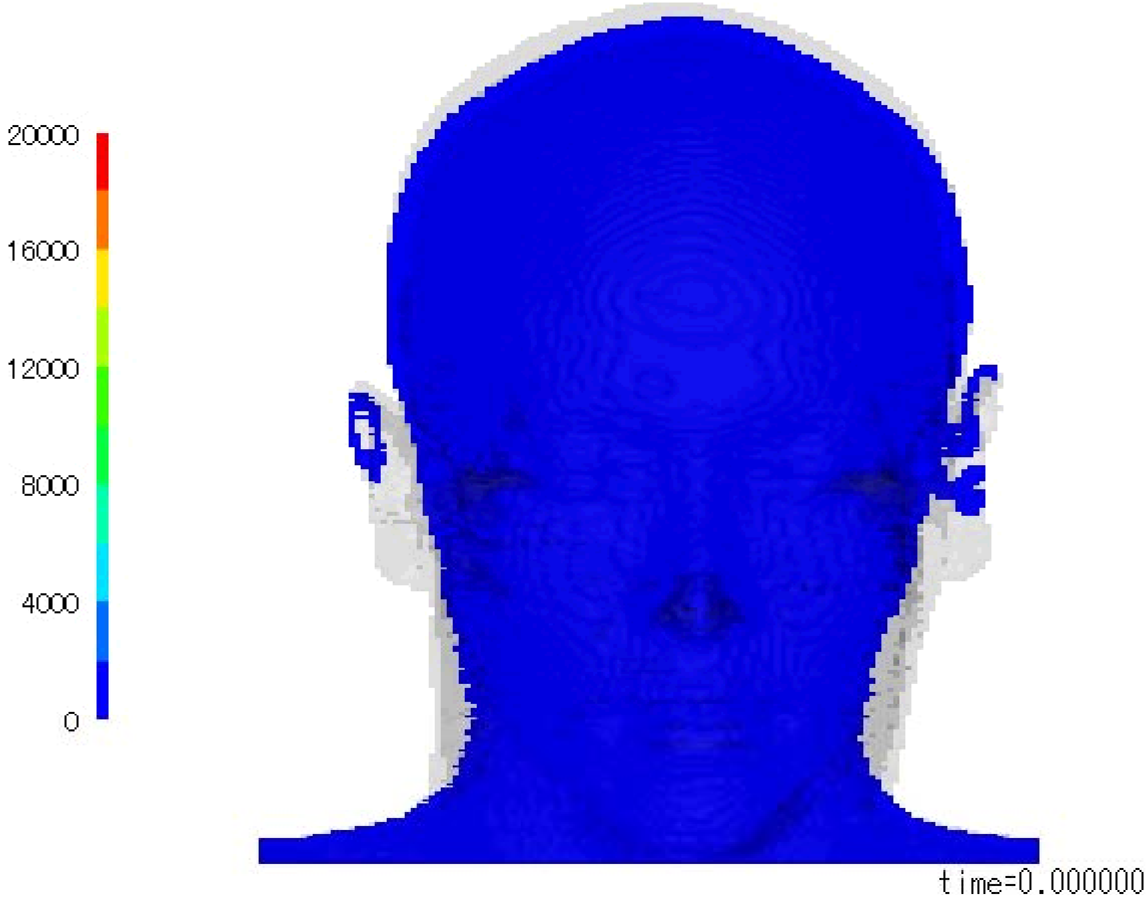

brain deformations: protection design

intelligent
shock absorption

three cases

- case 1: brain tissue (biomechanics)
- case 2: carnivorous plant (biology)
- case 3: semi-crystalline polymers (polymer physics)

viscoelastic deadly fluid in carnivorous plants

Laurence Gaume (Montpelier) & Yoel Forterre (Marseille)

the Nepenthes rafflesiana.

- Contains a fluid composed of water and polysaccharides

a fly tries to flee

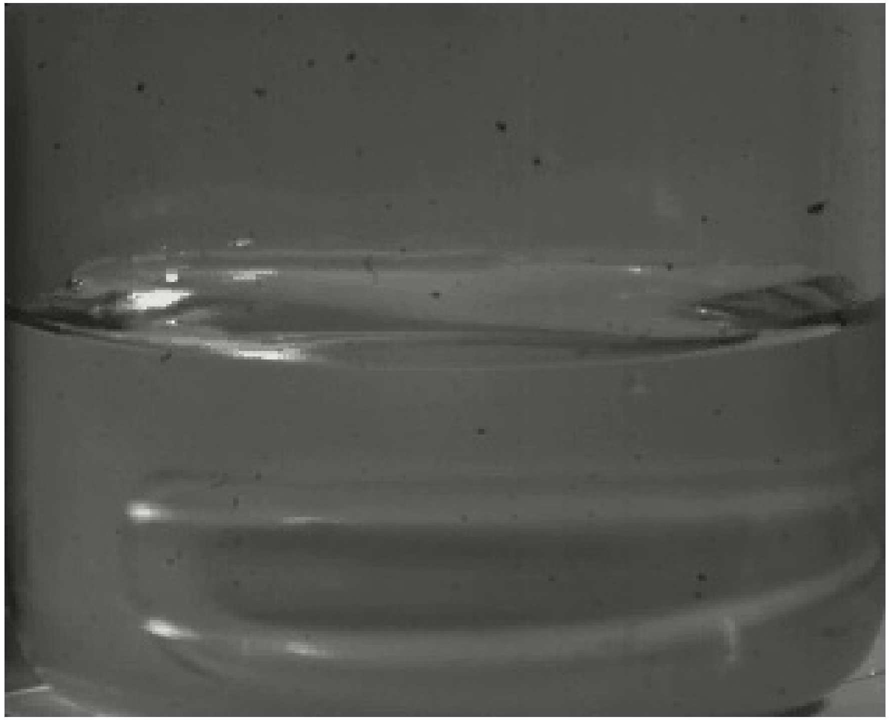

water

fluid

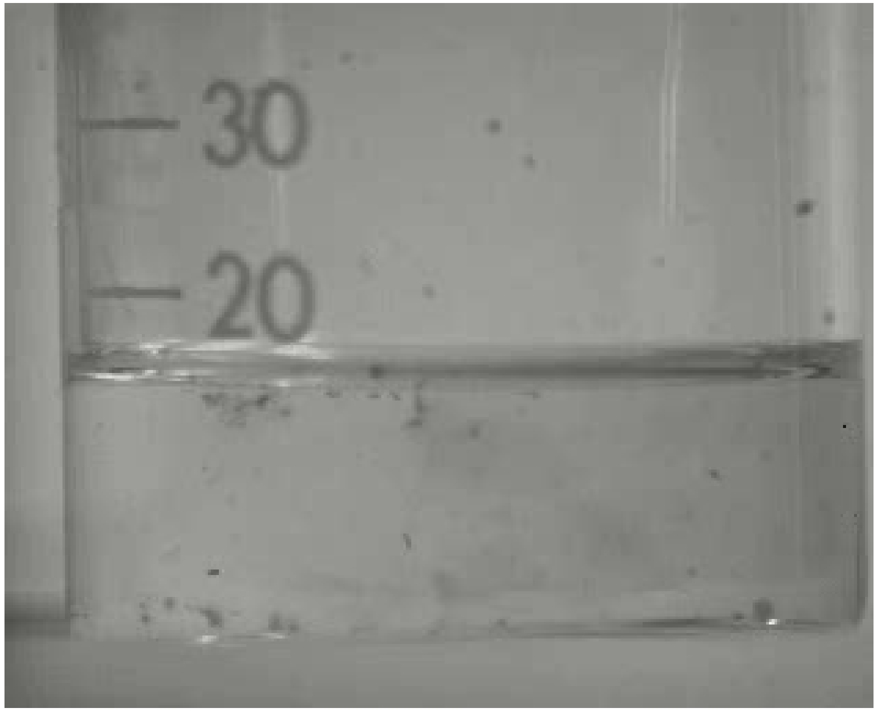

influence of concentration

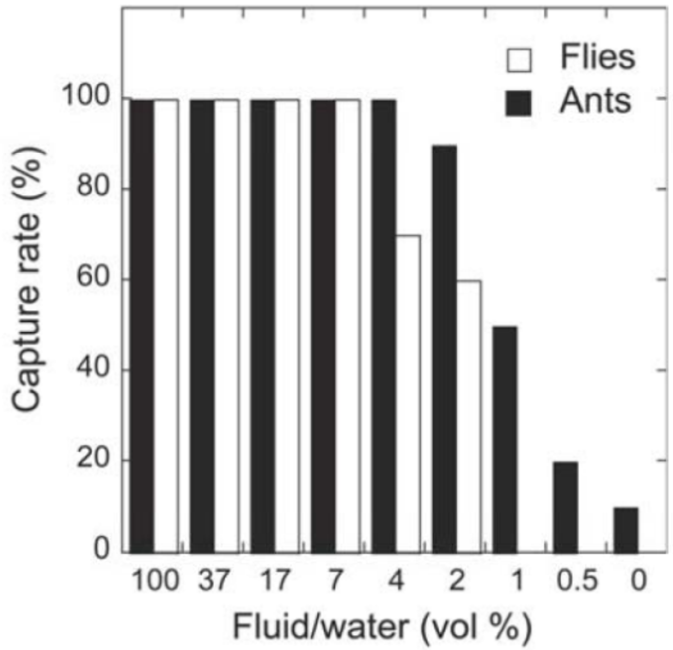

- it's not a chemical attack (insects recover when removed from the fluid)
- surface tension hardly varies with concentration: surface tension doesn't explain (σ_{fluid} = 0.0726 N.m, σ_{water} = 0.0720 N.m).

drag forces: viscosities of the pure fluid

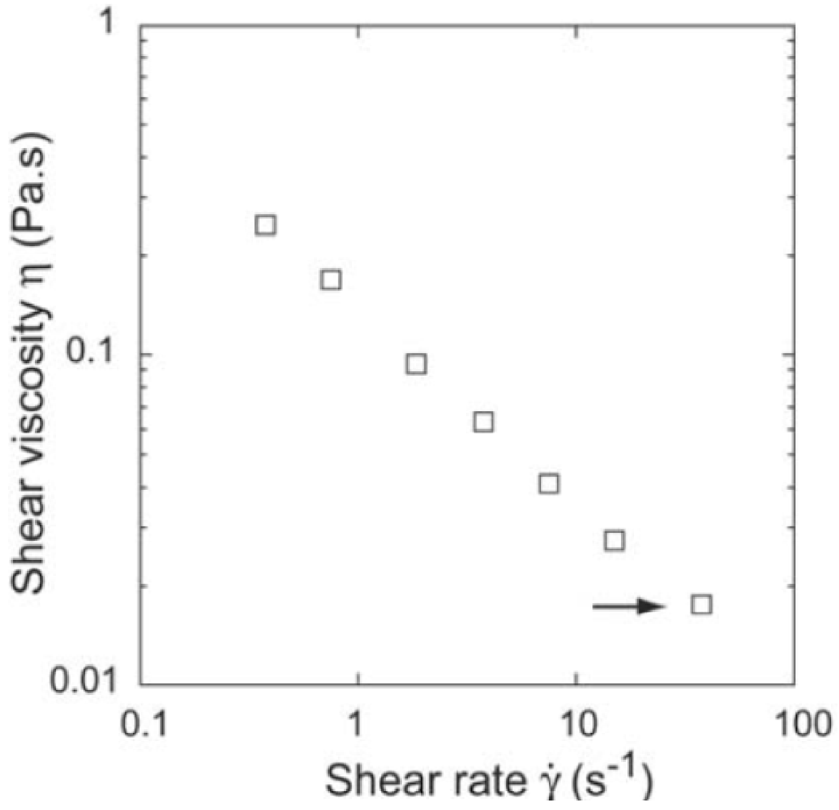

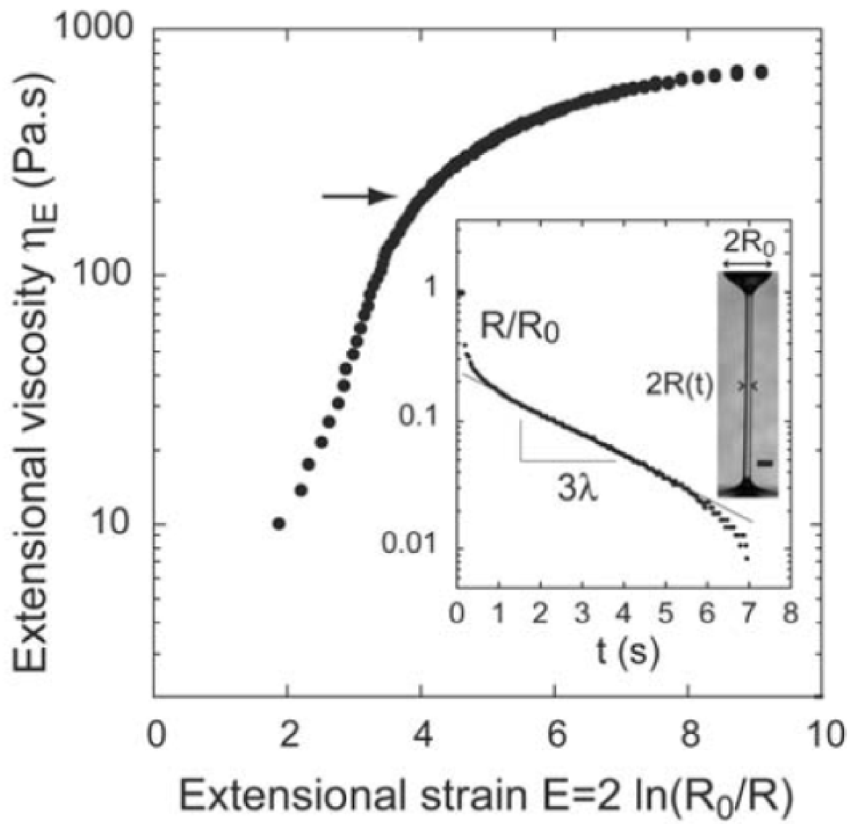

shear viscosity /shear rate (left)   transient extensional viscosity / strain (right)

arrows indicate typical values corresponding to insect motion in the fluid

elongational effects: filament formation

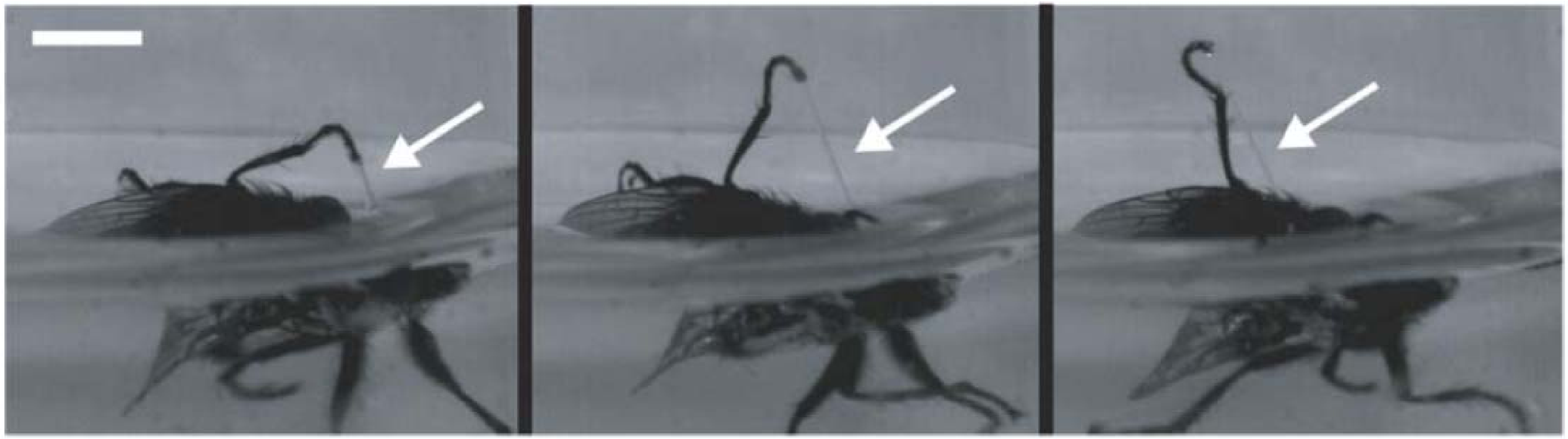

dynamical sequence of a fly in the digestive fluid showing a viscoelastic liquid filament attached to its leg (arrows)

viscosities: influence of concentration

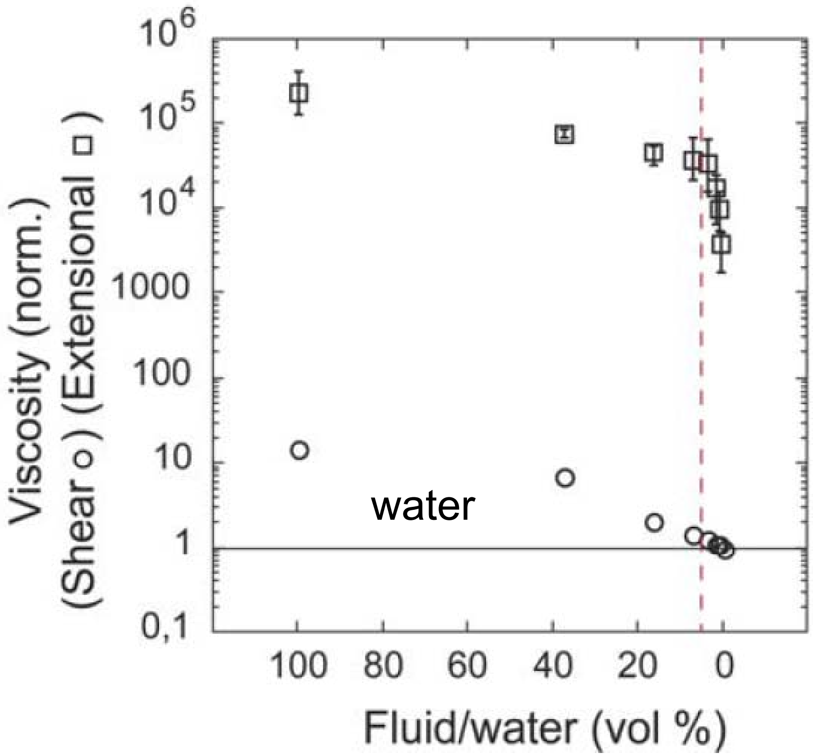

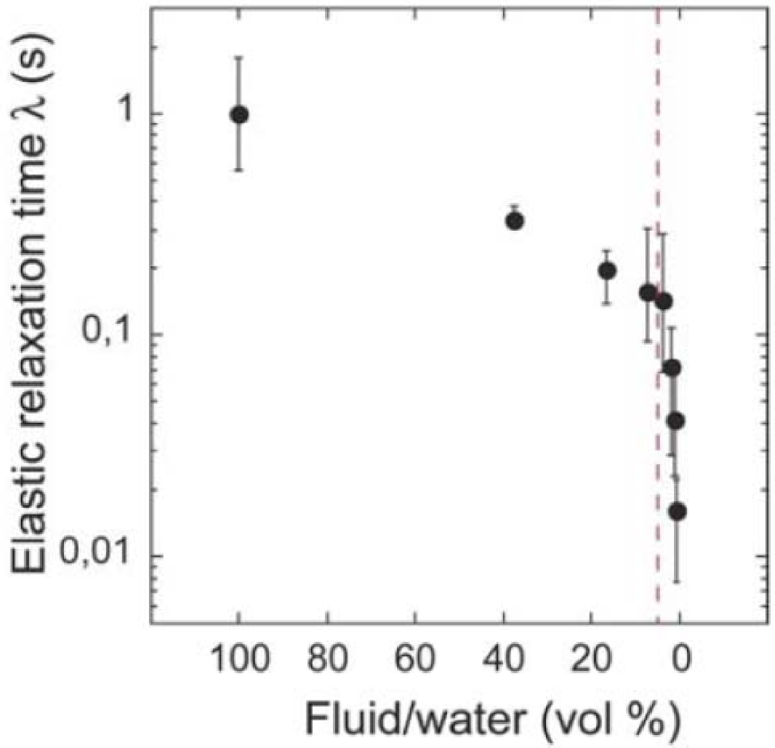

dilution effect on the shear (○) and extensional viscosity (□) (left)

dilution effect on the characteristic relaxation time (right)

capture rate versus De-number

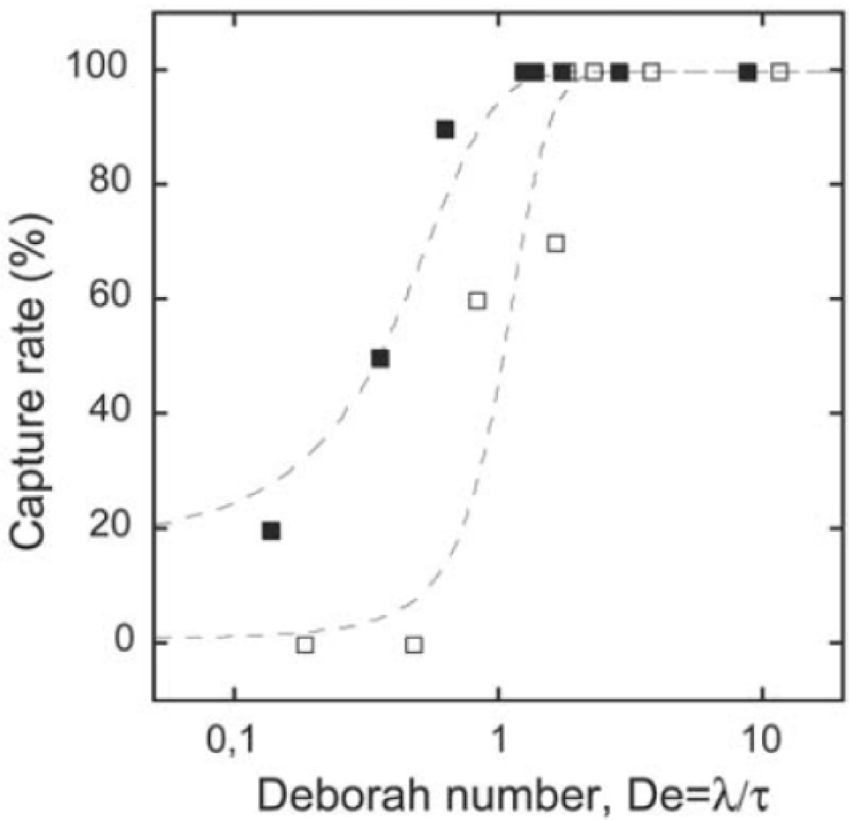

capture rate / Deborah number (flies □, ants ■)

-trapping efficiency is conditioned by both fluid viscoelasticity and insect dynamics

- tropical plants, often submitted to high rainfalls and thus variations in fluid concentration.

three cases

- case 1: brain tissue (biomechanics)
- case 2: carnivorous plant (biology)
- case 3: semi-crystalline polymers (polymer physics)

injection molding

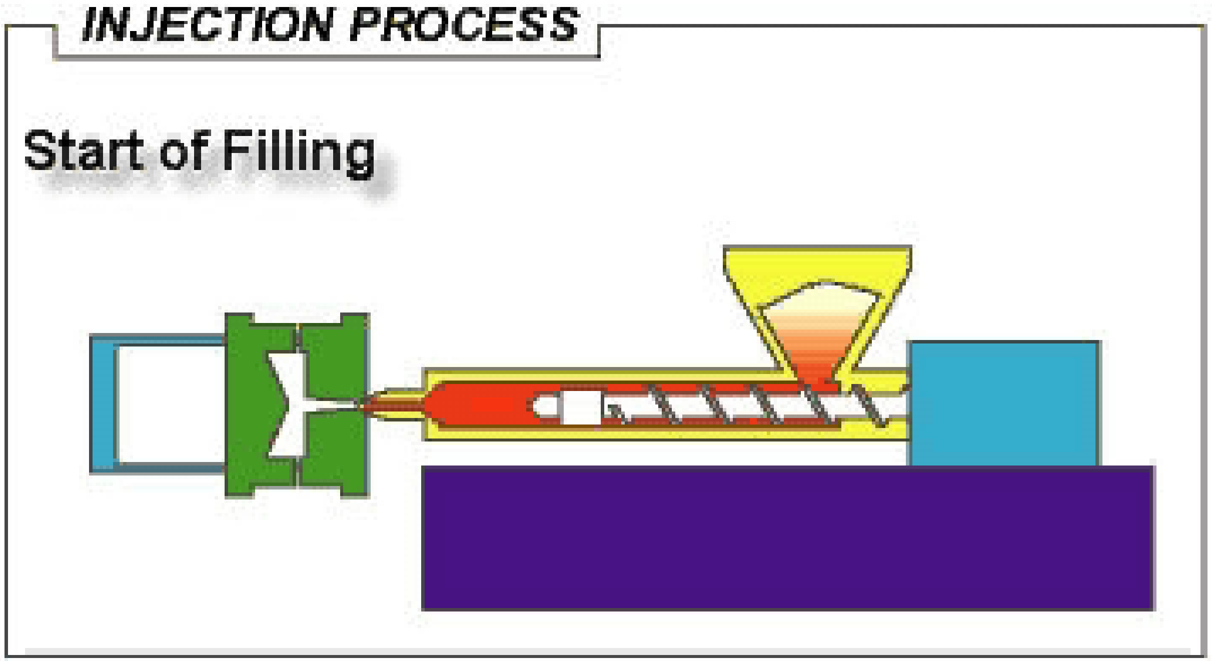

load-bearing applications of polymers

processing of semi-crystalline polymers

- Polymer processing:

  high $\dot{\gamma}$, high p and high $\dot{T}$ → structure formation

- Mechanical behaviour:
  - Influence of morphology

structure development during flow

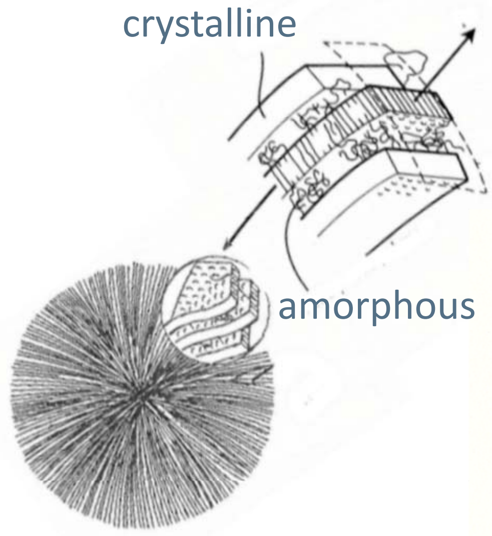

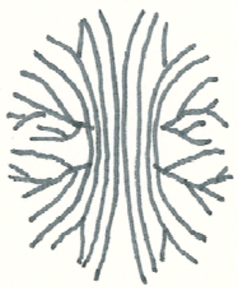

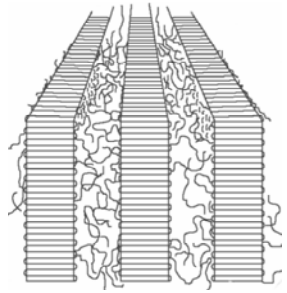

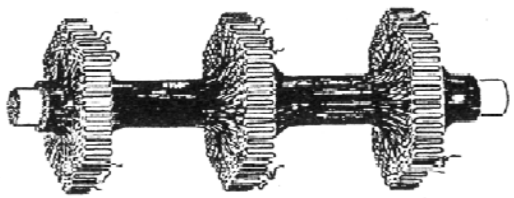

isotropic spherulites

slightly oriented spherulites

row structure

shish kebab

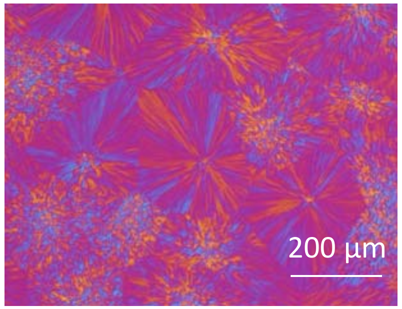

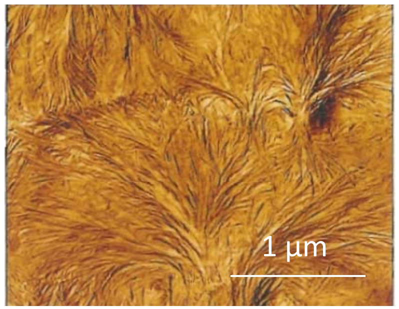

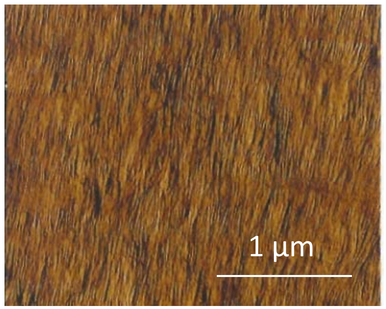

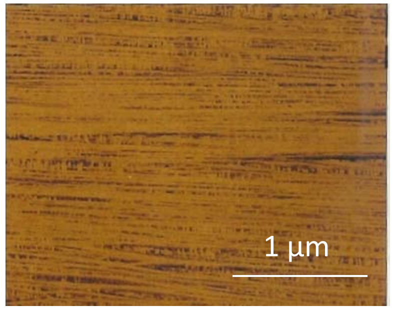

no orientation

strong orientation

flow

in-situ Small Angle X-ray Scattering (SAXS)

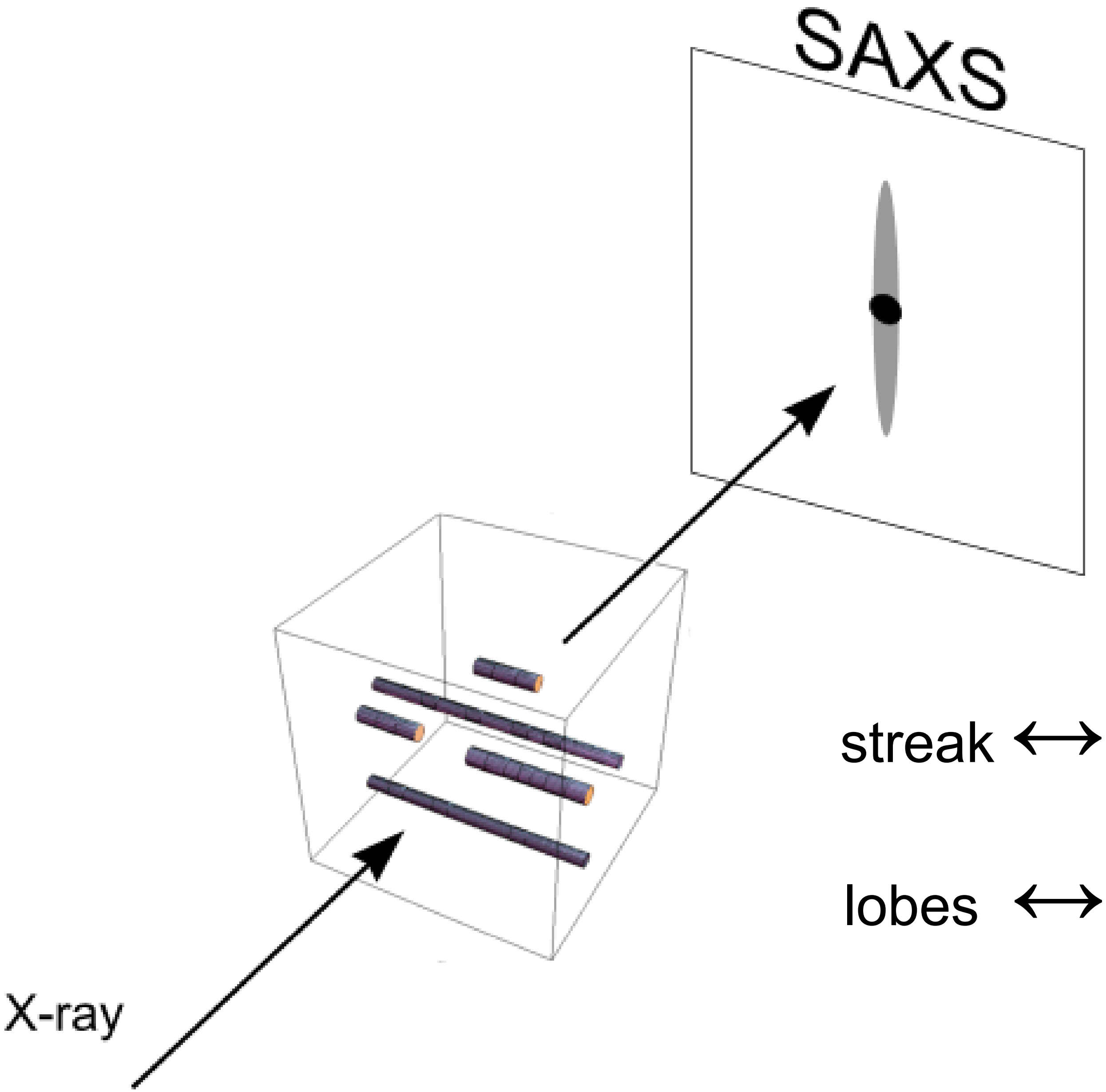

streak ⟷ fibrils

lobes ⟷ lamellae

in-situ: Small Angle X-ray Scattering (SAXS)

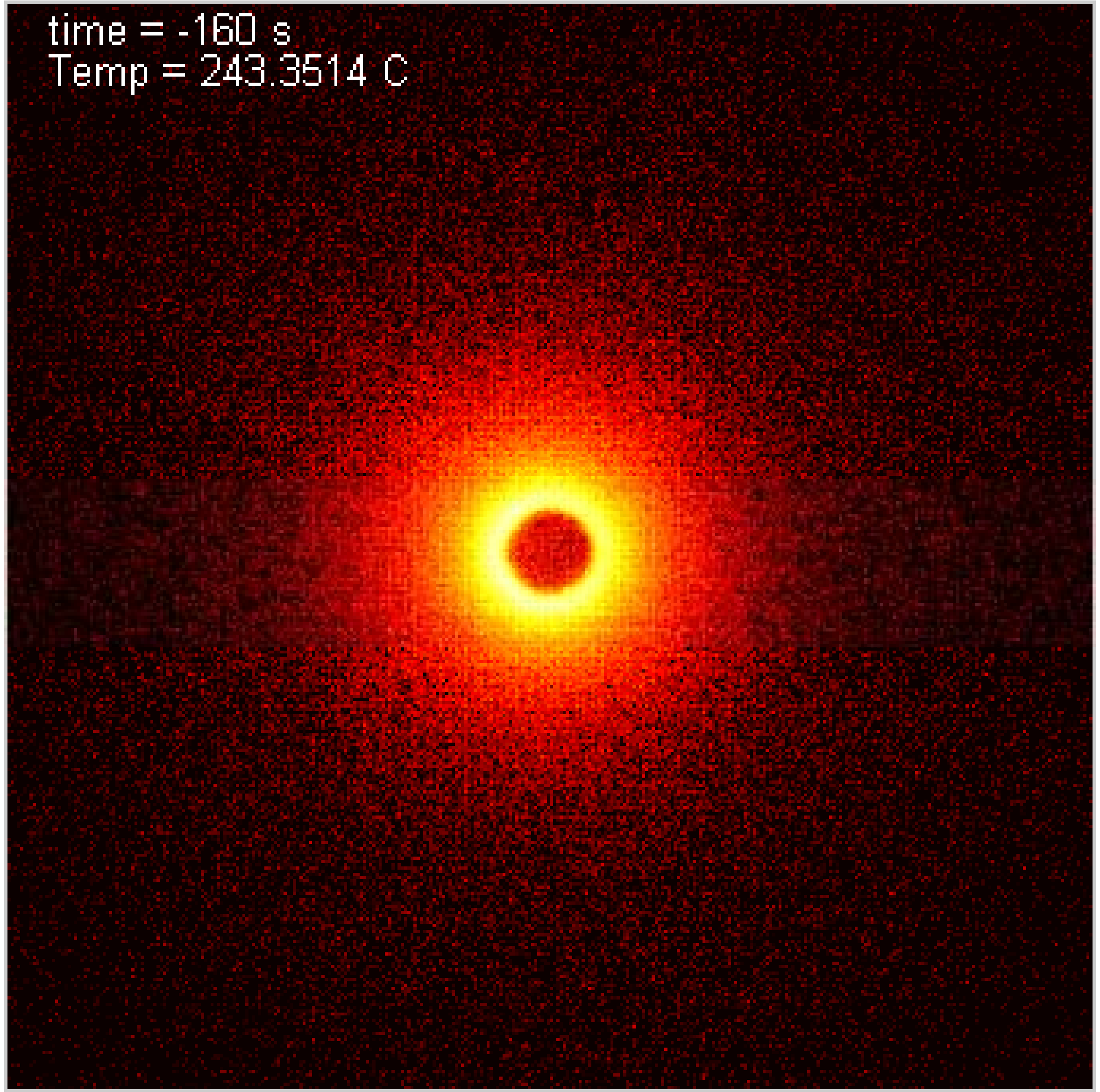

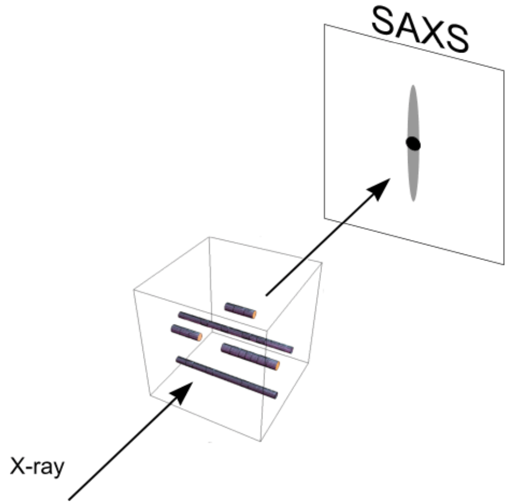

processing–structure–property

Injection molding of HDPE

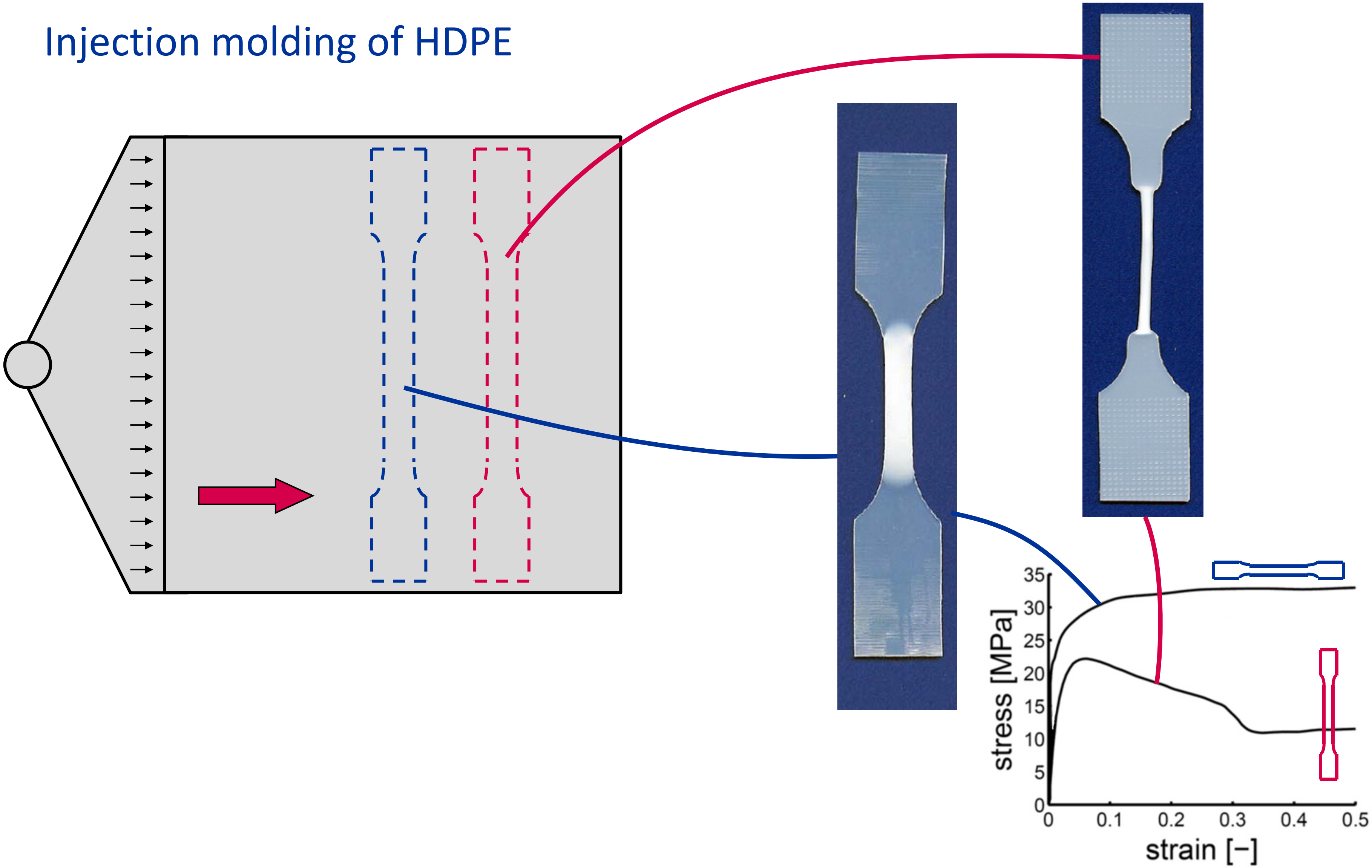

processing–structure–property: example (iPP)

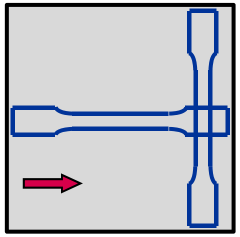

static load to failure

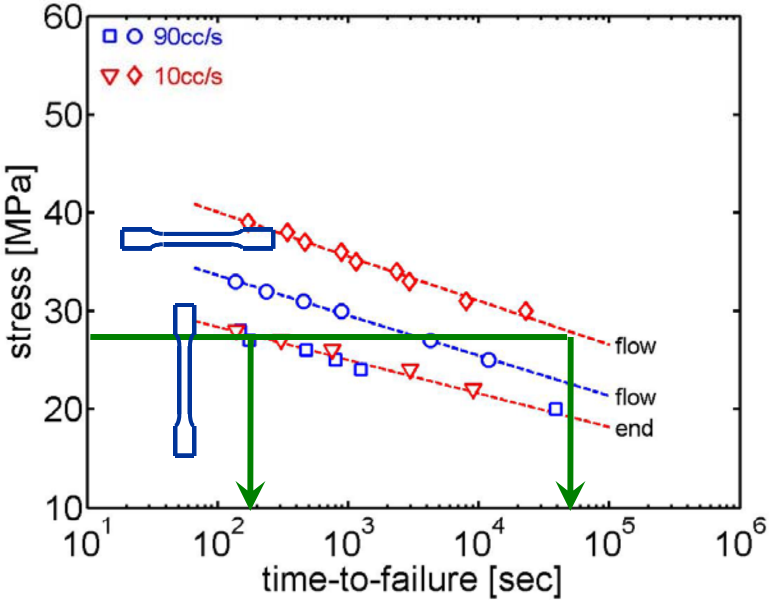

Factor 400 in lifetime for different positions/directions!

processing-structure-properties relations

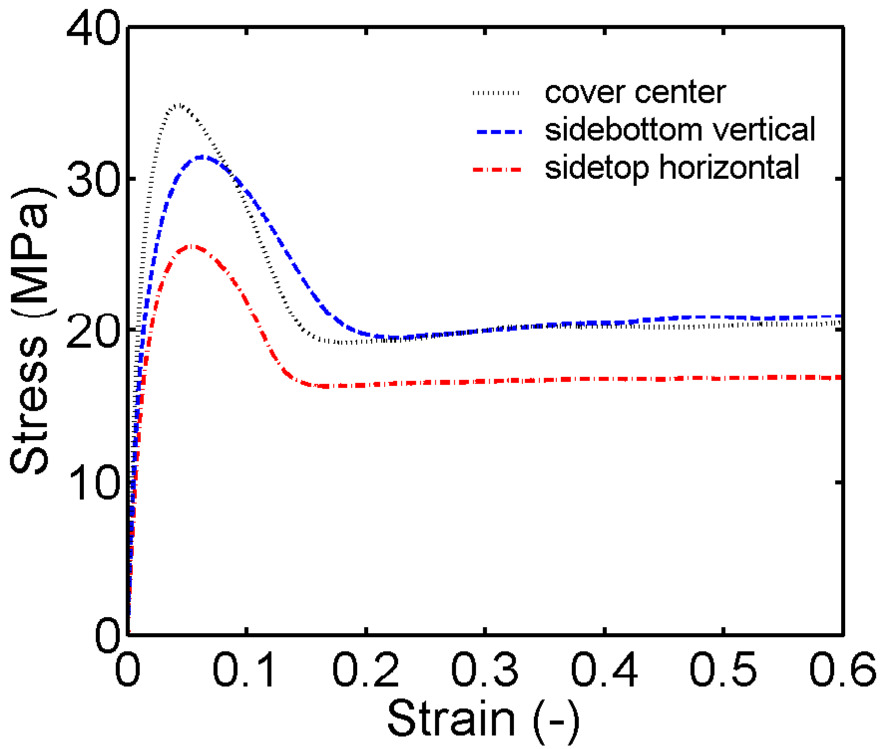

processing conditions: injection molding

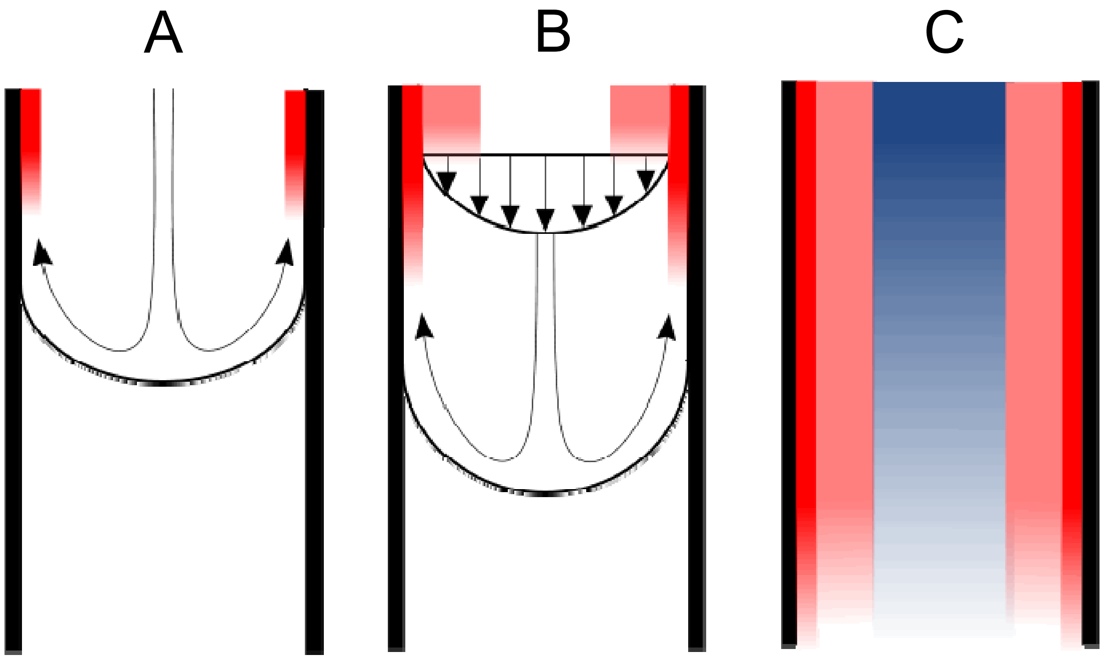

skin layer

rapid cooling
(~100 °C s^{-1})

shear layer

flow induced
crystallization
(~1000 s^{-1})

core layer

pressure induced
crystallization
(~1000 bar)

typical cross section of
semi-crystalline products

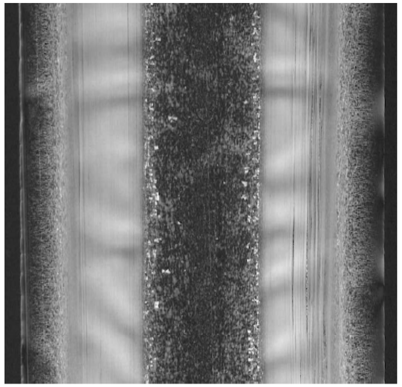

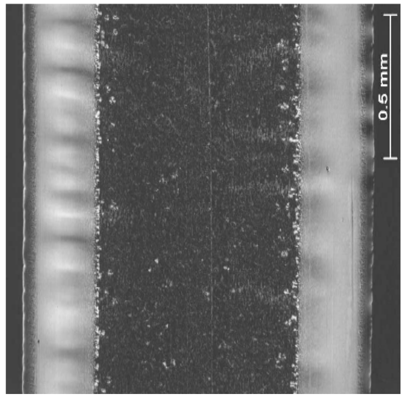

modeling flow effects on crystallization

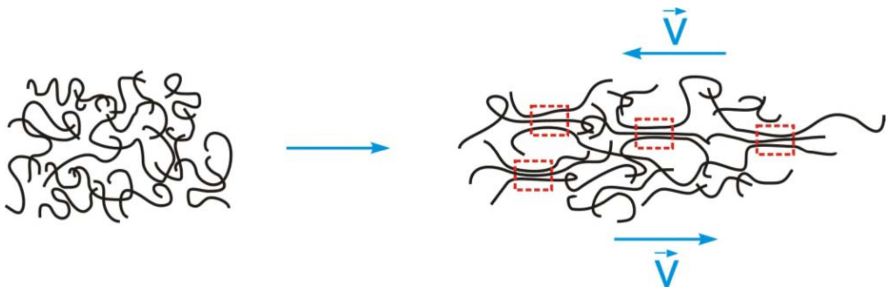

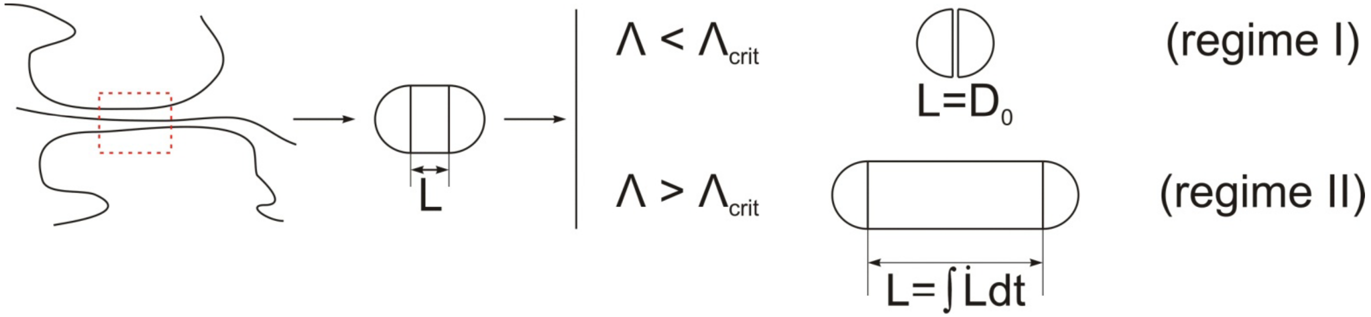

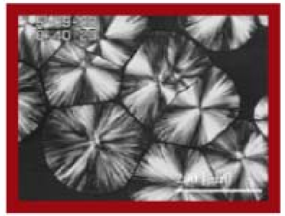

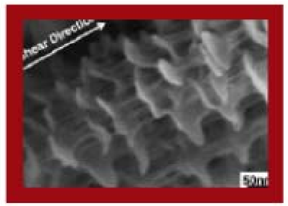

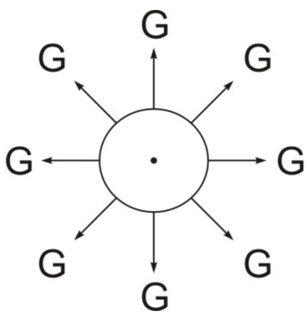

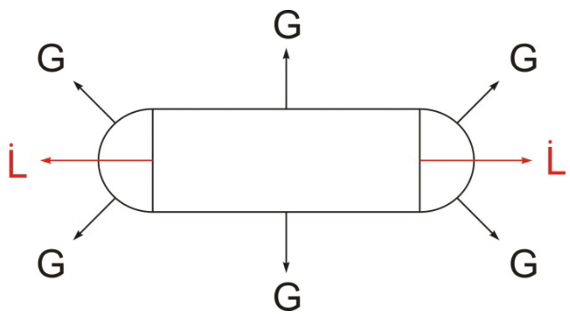

nonlinear viscoelasticity: the eXtended PomPom model

$$\overset{\nabla}{\boldsymbol{\tau}}_i + \boldsymbol{\lambda}(\boldsymbol{\tau}_i)^{-1} \cdot \boldsymbol{\tau}_i - 2G_i \boldsymbol{D} = \boldsymbol{0}$$

$$\alpha \neq 0 \rightarrow \Psi_2 \neq 0$$

$$\boldsymbol{\lambda}(\boldsymbol{\tau}_i)^{-1} = \frac{1}{\lambda_{b,i}} \left[\frac{\alpha_i}{G_i} \boldsymbol{\tau}_i + F(\boldsymbol{\tau}_i)\boldsymbol{I} + G_i \left(F(\boldsymbol{\tau}_i) - 1 \right) \boldsymbol{\tau}_i^{-1} \right]$$

$$\Lambda_i = \sqrt{1 + \frac{\operatorname{tr}(\boldsymbol{\tau}_i)}{3G_i}}$$

$$F(\boldsymbol{\tau}_i) = 2r_i e^{\frac{2}{q_i}(\Lambda_i - 1)} \left(1 - \frac{1}{\Lambda_i^2} \right) + \frac{1}{\Lambda_i^2} \left[1 - \frac{\alpha_i \operatorname{tr}(\boldsymbol{\tau}_i \cdot \boldsymbol{\tau}_i)}{3G_i^2} \right]$$

$$r_i = \frac{\lambda_{b,i}}{\lambda_{s,i}}$$

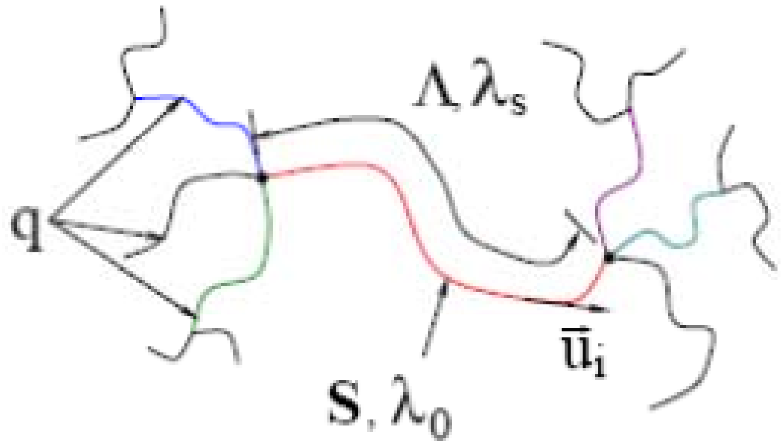

non-isothermal quiescent crystallization

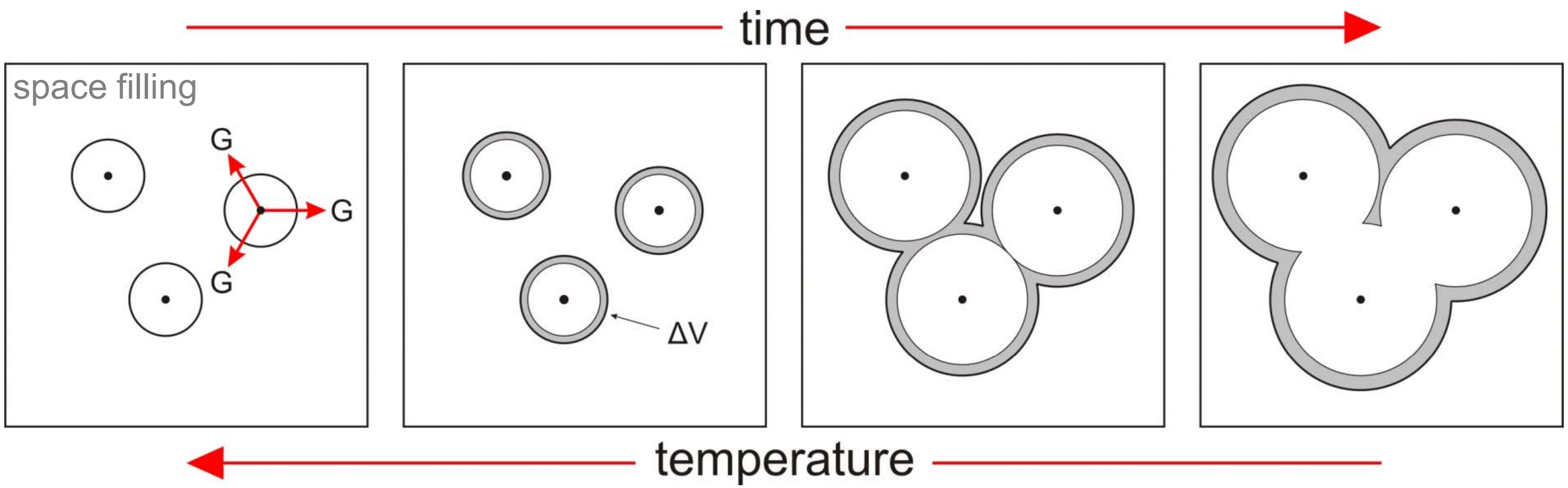

Schneider rate equations	$\dot{\phi}_3 = 8\pi\alpha$	$(\phi_3 = 8\pi N)$	'number'
	$\dot{\phi}_2 = G\phi_3$	$(\phi_2 = 4\pi R_{tot})$	'radius'
	$\dot{\phi}_1 = G\phi_2$	$(\phi_1 = S_{tot})$	'surface'
	$\dot{\phi}_0 = G\phi_1$	$(\phi_0 = V_{tot})$	'undisturbed volume'
Avrami equation	$-\ln(1-\xi) = \phi_0$		'real volume'
nucleation density	$N(T,p) = N_{\max} \exp\left[-c_N\left(T - T_{Nref}(p)\right)\right]$		
individual growth rate	$G_i(T,p) = G_{\max,i} \exp\left[-c_{G,i}\left(T - T_{Gref,i}(p)\right)^2\right]$		

flow-induced crystallization

total nucleation density	$N_{tot} = N_q + N_f$	
(flow-induced) nucleation rate	$\dot{N}_f = g_n \left(\Lambda_{hmw}^4 - 1 \right)$	
shish length (L) growth	$\dot{L} = g_l \left(\Lambda_{avg}^4 - 1 \right)$	for $\Lambda > \Lambda_{crit}$
rate equations	$\dot{\psi}_2 = 4\pi N_f \dot{L}$	'length'
	$\dot{\psi}_1 = G\psi_2$	'surface'
	$\dot{\psi}_0 = G\psi_1$	'undisturbed volume'
Avrami equation	$-\ln(1-\xi) = \phi_0 + \psi_0$	'real volume'

numerical simulation: no flow

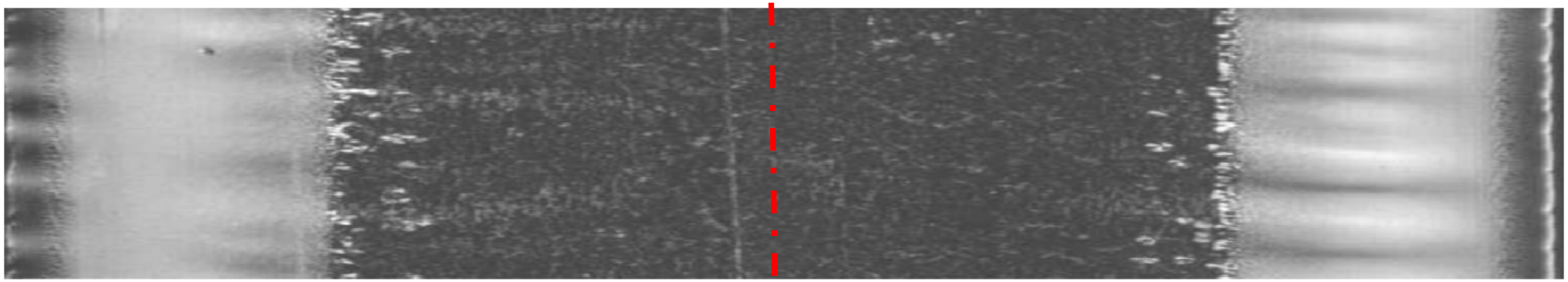

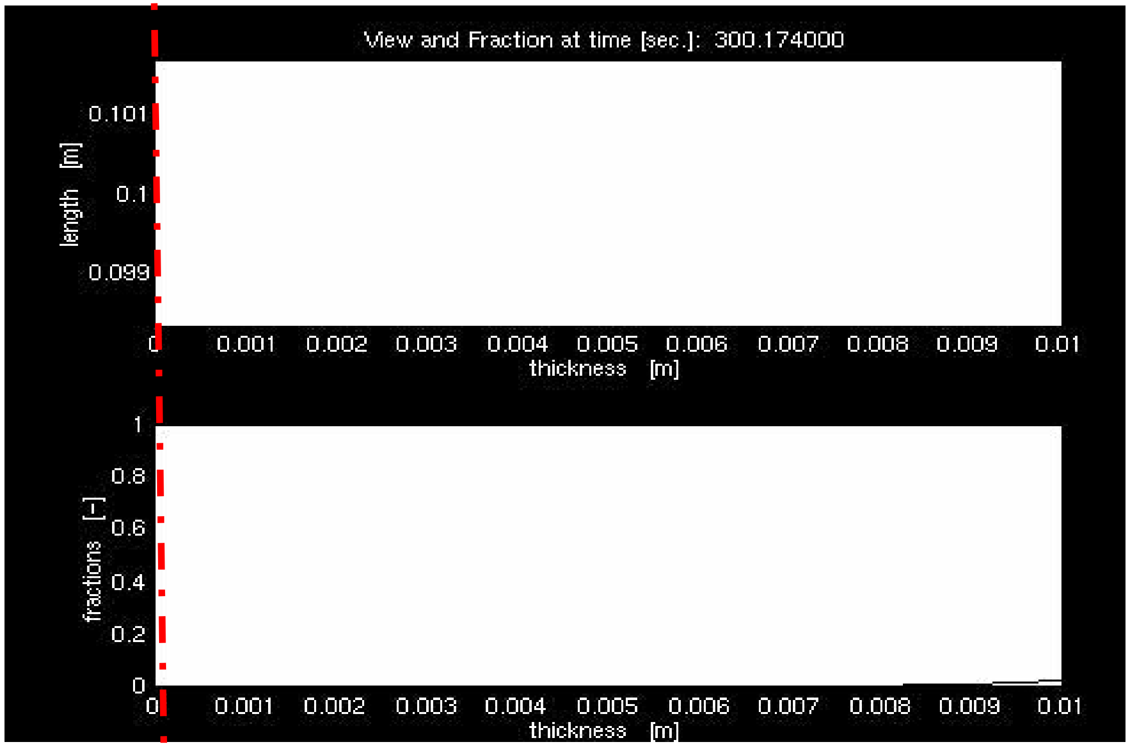

numerical simulation: flow

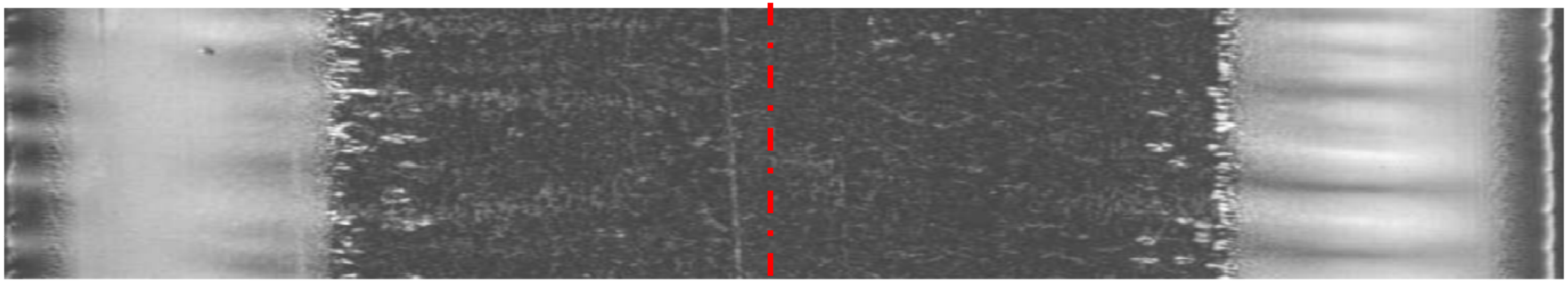

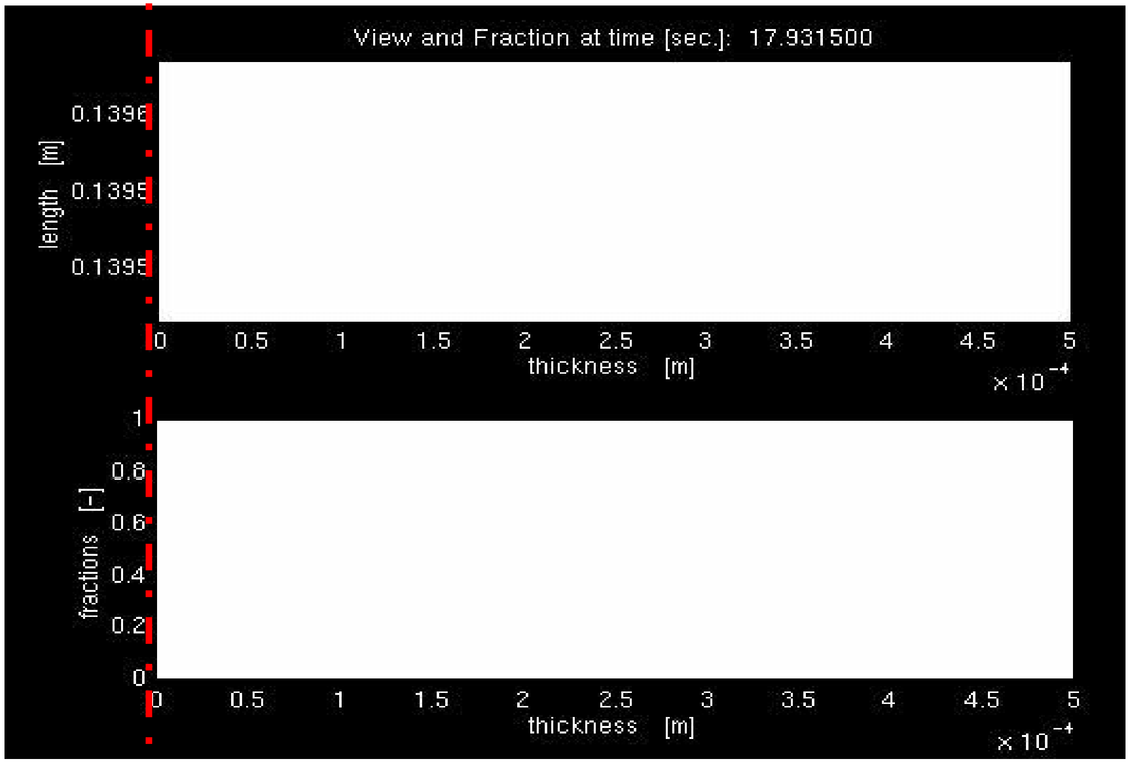

from processing conditions to structure

- use the experimental thermal and pressure history in the model

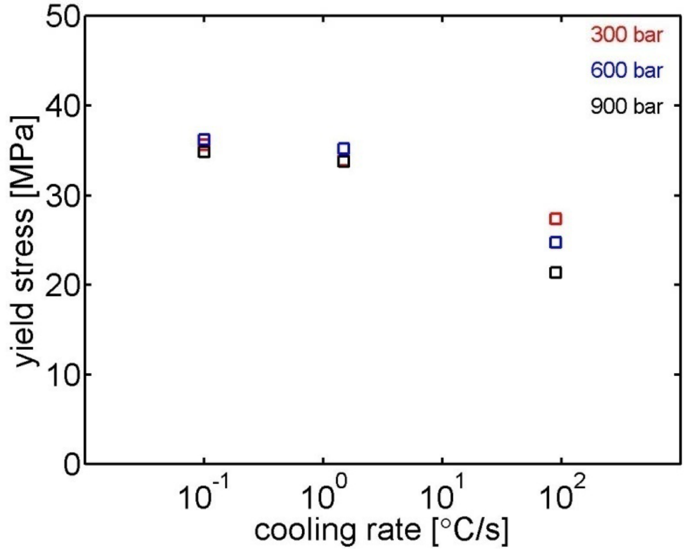

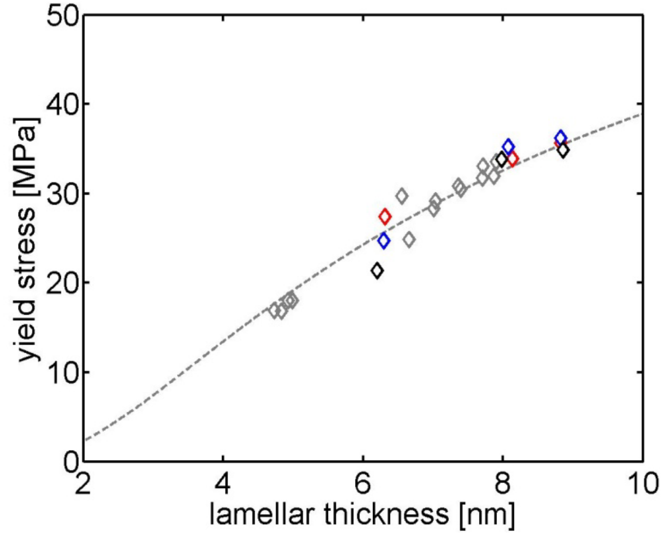

iPP

W.J. O'Kane, R.J. Young, Journal of Materials Science Letters, *14*, 433-435 (1995) so far for the real problems

acknowledgements

Tim van Erp

Martin van Dronge

Dario Cavallo

Luigi Balzano

Zhe Ma

Peter Roozemond

high pressure, in situ X-ray

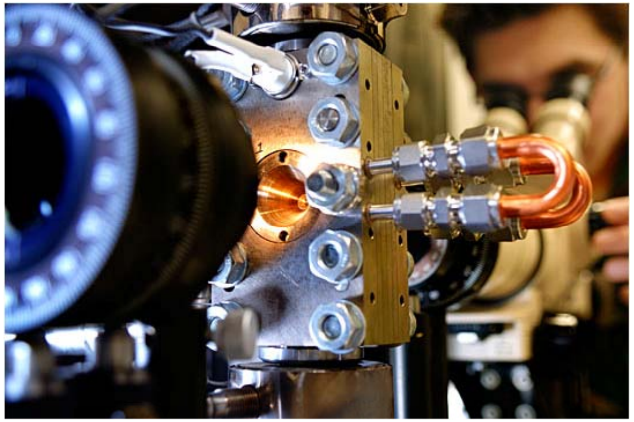

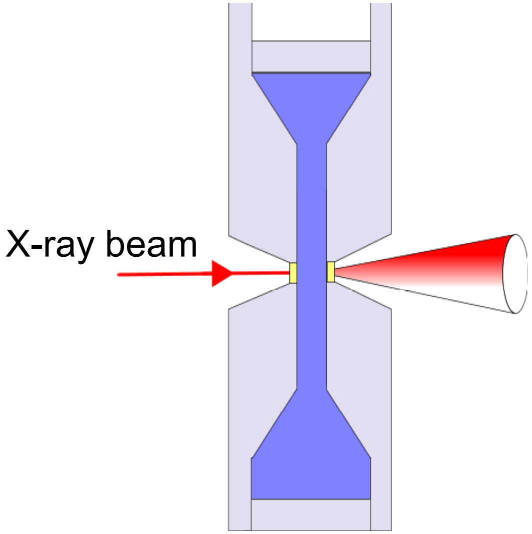

SAXS

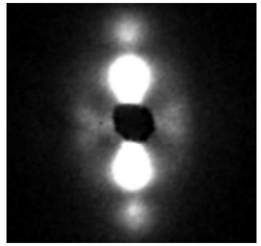

WAXD